

Erica J. Weiss and Martha Flanders

J Neurophysiol 92:523-535, 2004. First published Feb 18, 2004; doi:10.1152/jn.01265.2003

You might find this additional information useful...

This article cites 32 articles, 15 of which you can access free at:

<http://jn.physiology.org/cgi/content/full/92/1/523#BIBL>

This article has been cited by 17 other HighWire hosted articles, the first 5 are:

Identifying Representative Synergy Matrices for Describing Muscular Activation Patterns During Multidirectional Reaching in the Horizontal Plane

S. Muceli, A. T. Boye, A. d'Avella and D. Farina
J Neurophysiol, March 1, 2010; 103 (3): 1532-1542.

[\[Abstract\]](#) [\[Full Text\]](#) [\[PDF\]](#)

Stability of muscle synergies for voluntary actions after cortical stroke in humans

V. C. K. Cheung, L. Piron, M. Agostini, S. Silvoni, A. Turolla and E. Bizzi
PNAS, November 17, 2009; 106 (46): 19563-19568.

[\[Abstract\]](#) [\[Full Text\]](#) [\[PDF\]](#)

Simplified and effective motor control based on muscle synergies to exploit musculoskeletal dynamics

M. Berniker, A. Jarc, E. Bizzi and M. C. Tresch
PNAS, May 5, 2009; 106 (18): 7601-7606.

[\[Abstract\]](#) [\[Full Text\]](#) [\[PDF\]](#)

Effects of Object Compliance on Three-Digit Grasping

S. A. Winges, S. E. Eonta, J. F. Soechting and M. Flanders
J Neurophysiol, May 1, 2009; 101 (5): 2447-2458.

[\[Abstract\]](#) [\[Full Text\]](#) [\[PDF\]](#)

Discharges in Human Muscle Receptor Afferents during Block Grasping

M. Dimitriou and B. B. Edin
J. Neurosci., November 26, 2008; 28 (48): 12632-12642.

[\[Abstract\]](#) [\[Full Text\]](#) [\[PDF\]](#)

Updated information and services including high-resolution figures, can be found at:

<http://jn.physiology.org/cgi/content/full/92/1/523>

Additional material and information about *Journal of Neurophysiology* can be found at:

<http://www.the-aps.org/publications/jn>

This information is current as of May 14, 2010 .

Muscular and Postural Synergies of the Human Hand

Erica J. Weiss and Martha Flanders

Department of Neuroscience, University of Minnesota, Minneapolis, Minnesota 55455

Submitted 29 December 2003; accepted in final form 16 February 2004

Weiss, Erica J. and Martha Flanders. Muscular and postural synergies of the human hand. *J Neurophysiol* 92: 523–535, 2004. First published February 18, 2004; 10.1152/jn.01265.2003. Because humans have limited ability to independently control the many joints of the hand, a wide variety of hand shapes can be characterized as a weighted combination of just two or three main patterns of covariation in joint rotations, or “postural synergies.” The present study sought to align muscle synergies with these main postural synergies and to describe the form of membership of motor units in these postural/muscle synergies. Seventeen joint angles and the electromyographic (EMG) activities of several hand muscles (both intrinsic and extrinsic muscles) were recorded while human subjects held the hand statically in 52 specific shapes (i.e., shaping the hand around 26 commonly grasped objects or forming the 26 letter shapes of a manual alphabet). Principal-components analysis revealed several patterns of muscle synergy, some of which represented either coactivation of all hand muscles, or reciprocal patterns of activity (above and below average levels) in the intrinsic index finger and thumb muscles or (to a lesser extent) in the extrinsic four-tendoned extensor and flexor muscles. Single- and multiunit activity was generally a multimodal function of whole hand shape. This implies that motor-unit activation does not align with a single synergy; instead, motor units participate in multiple muscle synergies. Thus it appears that the organization of the global pattern of hand muscle activation is highly distributed. This organization mirrors the highly fractured somatotopy of cortical hand representations and may provide an ideal substrate for motor learning and recovery from injury.

INTRODUCTION

Finger movement is a fascinating topic with a growing basic science literature and potential applications in prosthetics and rehabilitation. The best-studied aspects are the control of the intrinsic muscles of the index finger and thumb in pinching (Huesler et al. 2000; Johanson et al. 2001; Maier and Hepp-Reymond 1995a,b; Valero-Cuevas 2000), the role of compartmentalization of the extrinsic, four-finger flexors and extensors in the control of individuation (Keen and Fuglevand 2004; Kilbreath and Gandiviva 1994; Reilly and Schieber 2003), and the temporal coordination of the index finger and thumb during reaching/grasping movements (Paulignan et al. 1997). Due to the complexity, however, fewer studies have sought to examine the coordination of intrinsic and extrinsic hand muscles in controlling the shape of the entire hand (see Santello et al. 2002; Schieber 1995).

Although global patterns of hand muscle coordination have yet to be explored, global patterns of force and movement have been described in several recent papers. Even the most dexterous humans cannot achieve fully independent forces or movements of the four fingers: there is substantial coupling across

adjacent fingers (Hager-Ross and Schieber 2000; Rearick et al. 2003; Santello and Soechting 2000). In our laboratory, patterns of coupling and covariation have been studied by using an instrumented glove to record ≤ 17 joint angles (including 2 or 3 angles for each finger and 4 for the thumb). A reduction in degrees of freedom was documented by applying principal-components analysis to the sets of joint angles that represented large numbers of complex hand shapes. Only two principal components (PCs) were needed to account for $>80\%$ of the variance in a set of hand shapes for 57 commonly grasped objects (Santello et al. 1998). Although these objects ranged from a baseball (power grip) to a needle (precision grip), because the behavior was confined to grasping, it was not entirely surprising to find just two main axes along which sets of joints together showed extension-flexion or abduction-adduction. It was somewhat more surprising to discover that just three or four axes captured the main features of the 26 visually distinct letters of the American Sign Language (ASL) manual alphabet (Jerde et al. 2003a).

In the present study, we capitalized on this recent discovery of a concise system for representing complex hand postures. The main goal of our investigation was to examine multi- and single-unit electromyographic (EMG) activity as a function of hand shape. We recorded from a set of intrinsic and extrinsic hand muscles as each subject held 52 specific hand shapes. We then computed EMG principal component axes (the “muscle synergies”) and found the two orthogonal hand-shape axes that were best aligned with the most common muscle synergies. This allowed us to examine patterns of membership of muscles and motor units in muscular and postural synergies.

METHODS

Instructions to subjects

In the first part of our study (referred to as “grasping” or “G”), four comfortably seated human subjects were asked to mold their right hands around 26 common tools, toys, or other useful objects. We assembled this group of objects on tables around the subject, and we asked each subject to practice until he or she felt that they could produce consistent hand shapes over repeated trials with a given item. The objects, which are listed in Fig. 1A, were given an alphabetical code from A (for “A tool,” which was a pair of pliers) to Z (for zipper). We stressed to subjects that while their fingertips should lightly touch the object (as if they were about to use it), they were not allowed to produce force against it. Instead, it was imperative that all of the force produced by their hand muscles went into holding the hand in a specific static posture. The weight of the object was either supported by the table or by the subject’s other hand.

In the second part of our study (referred to as “spelling,” or “L” for

Address for reprint requests and other correspondence: M. Flanders, Dept. of Neuroscience, 6–145 Jackson Hall, 312 Church St. S.E., University of Minnesota, Minneapolis MN 55455 (E-mail: fland001@umn.edu).

The costs of publication of this article were defrayed in part by the payment of page charges. The article must therefore be hereby marked “advertisement” in accordance with 18 U.S.C. Section 1734 solely to indicate this fact.

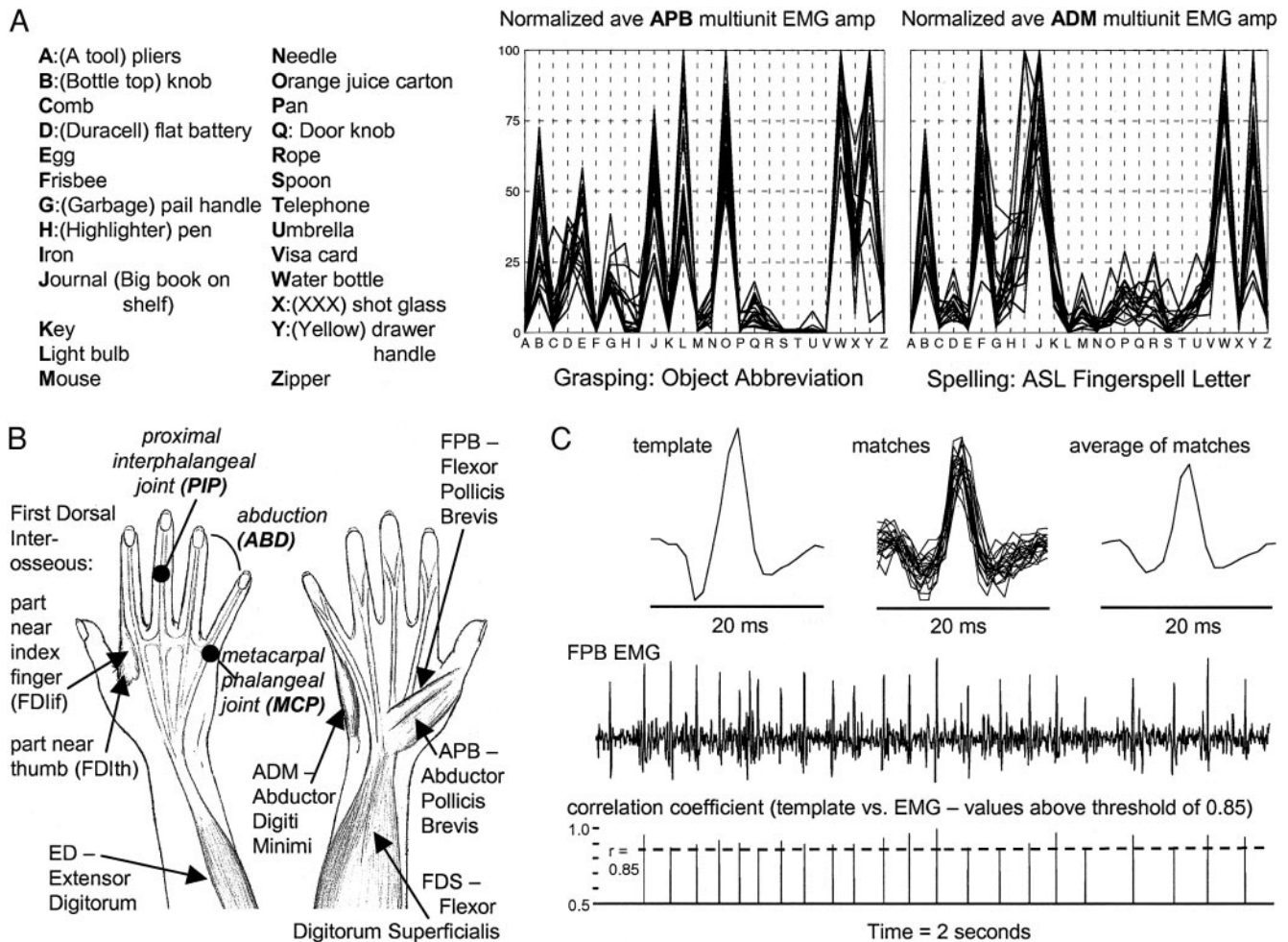


FIG. 1. **A:** list of 26 grasped objects and examples of normalized multiunit electromyographic (EMG) amplitudes. The grasped objects were given an alphabetical code, from A (for “A tool”) to Z (for zipper). Subjects did not produce force against the object; instead the muscular activity was used to shape the hand. Each experiment was conducted in sequential blocks of 26 trials, and EMG levels were normalized to the maximum in each block. *Left:* the activity of abductor pollicis brevis (APB) for *subject 3*’s grasping experiment (G3). *Right:* the activity of abductor digiti minimi (ADM) for *subject 1*’s spelling experiment (L1). **B:** anatomical locations of the 7 muscles or muscle parts. A pair of bipolar surface electrodes was attached to the skin over each of 5 muscles, and 2 pairs were placed over the first dorsal interosseous (FDI). An instrumented glove was used to measure 17 joint angles including the proximal interphalangeal (PIP) and metacarpal-phalangeal (MCP) joints and the angle of abduction (ABD) between fingers. **C:** an example of our template matching for the identification of a single motor unit. A multiunit surface EMG recording is shown for a 2-s-long trials where *subject 4* lightly grasped the handle of an iron. A unit template (*top left*) was correlated with the EMG trace at each point in time, and the unit was discriminated (vertical lines) only at times when the correlation coefficient exceeded a threshold level of 0.85 (horizontal dashed line). *Top middle and left:* all of the matches in this trial and an average that could be used to update the template.

letter), in separate recording sessions, the same four subjects held their right hands in the 26 letter shapes of the ASL manual alphabet. Although none of the subjects were fluent signers, they were given ample opportunity to practice, and our previous research has indicated that novices are able to produce the same static hand shapes as professionals (Jerde et al. 2003a). Again the subjects were instructed that all of the force produced by hand muscles should go into holding the hand in specific static postures. In this case, the instruction was to avoid producing forces against other digits while holding the more closed letter shapes (e.g., E, M, N, S, T, X).

Three of the subjects were right-handed women and one was a left-handed man (performing with his right hand). All were neurologically normal and gave informed consent. Each subject grasped or spelled each object or letter 16 times. Presentation order was randomized within the 16 blocks of 26 trials in each session for a total of 416 grasping trials and 416 spelling trials. The only exception was the spelling experiment with *subject 4* (experiment

L4), where there were only eight repeats of each letter, for a total of 208 trials (see Table 1).

Data acquisition

HAND SHAPE. Subjects wore a right-handed glove (Cyberglove, Virtual Technologies, Palo Alto, CA). The glove was open at the fingertips and was individually calibrated for each subject using a standard set of postures. We recorded from 17 sensors with an angular resolution of $<0.5^\circ$ and a temporal resolution of 12 ms. These data were subsequently averaged across 1 s. The measured angles were: the metacarpal phalangeal (MCP) and proximal interphalangeal (PIP) joint angles for the thumb and four fingers, abduction (ABD) of the thumb, middle, ring, and little fingers, thumb rotation (ROT), and wrist pitch and yaw. Some of these joints and angles are indicated in Fig. 1B. For viewing the results, we sometimes converted the Cyberglove data into a picture of the hand shape. Images were rendered

TABLE 1. Percent of trials where discriminant analysis provided correct identification of the grasped object or spelled letter

	17 Joint Angles		7 EMG Levels	
	Grasp, %	Spell, %	Grasp, %	Spell, %
Subject 1	88	93	44	63
Subject 2	87	93	46	56
Subject 3	89	95	49	41*
Subject 4	77	80	37	33†

Chance level was 3.9% (for 26 objects or letters). EMG, electromyogram. * For subject 3 spelling, only 6 muscles were used (because the flexor pollicis brevis electrode became detached during the experiment). † Subject 4 spelling was the first experiment conducted and according to the initial design, only 6 muscles were used (excluding abductor digiti minimi) and there were only 8 repeats instead of 16.

using Persistence of Vision Ray Tracer (POV-Ray, copyrighted free-ware).

MUSCLE ACTIVITY. During each experiment, we recorded seven channels of EMG activity. For simplicity, we will refer to these seven channels as representing seven “muscles,” even though two of the channels were associated with different recording locations on the same muscle and many of the channels were expected to also record smaller signals from neighboring muscles. Muscle activity was recorded for 2 s during the static holding phase of each trial.

We used custom-made adhesive fittings to attach small bipolar Ag/AgCl electrodes to the skin. The conductive surfaces were 2 mm in diameter, and the disk centers were positioned 1 cm apart. As indicated in Fig. 1B, these electrodes were placed over abductor pollicis brevis (APB), flexor pollicis brevis (FPB), the portion of the first dorsal interosseus closer to the index finger (FDI_{if}), the portion of the first dorsal interosseus closer to the thumb (FDI_{th}), extensor digitorum (ED), abductor digiti minimi (ADM), and flexor digitorum superficialis (FDS). APB and FPB are intrinsic muscles of the thumb. FDI and ADM are intrinsic muscles of the index and little fingers, respectively. ED and FDS are extrinsic hand muscles with their bellies in the forearm and four long tendons inserting on the middle to distal (ED) or middle (FDS) phalanges of the four fingers. The electrodes were placed approximately over the middle portion of each of these muscles. For FDS, we aimed to place the electrodes closest to the ring finger portion, but we did not attempt to isolate it with test maneuvers. As discussed in the following text, the spatial relationship between the electrode and the muscle may vary with hand and wrist posture. Muscle activity was amplified, band-pass filtered (60–500 Hz) and digitized at 1,000 samples/s.

Data analysis

PROCESSING EMG SIGNALS. We took two complementary approaches to measuring the “amount” of activity recorded on each channel during each trial. As shown in Figs. 1C and 3, the EMG record generally captured the steady-state firing of several motor units as reflected in the overall amplitude of the signal. Thus the metric for multiunit activity was the average amplitude of the rectified signal. This amplitude measurement is unavoidably contaminated by postural variations in the exact distance between the electrodes and the active units (due to muscle contraction and skin stretching) and, to a lesser extent, by the activities of neighboring muscles. To control for these problems we also quantified the firing rates of identified single motor units within as many of the records as possible. As described in the following text, unit identification was resistant to variations in the recorded amplitudes of motor unit potentials. Moreover, an identifiable single motor unit is almost certainly located very close to the recording electrode and is, by definition, confined to a single muscle or compartment. However, unit identification has its own limitations

(e.g., waveform superposition in trials with high activity levels), and it was not successful for all subjects and muscles. Therefore the single-unit data will mainly be presented for comparison with the multiunit results.

To estimate the level of activity in multiple units, we rectified the signal and took the average value across the 2-s interval. As shown in Fig. 1A, within each consecutive set of 26 trials (objects or letters), these average multiunit EMG amplitudes were then normalized so that the peak activity in that set was 100 and the minimum activity was 0. This normalization procedure adjusted for instances where (perhaps due to hand temperature or sweating within the glove) the EMG amplitude gradually changed as a function of time during the 2 h of the experiment.

We estimated the firing rate (spikes per second) of each discriminated single motor unit using a custom-written template-matching program. As shown in Fig. 1C, this program cross-correlated the EMG record with a template motor-unit waveform chosen from one of the first trials. This procedure is similar to a wavelet analysis at a single scale (Flanders 2002) except that the “wavelet” was a specific motor-unit potential and a threshold was applied. Thus spikes were accepted only when the correlation coefficient was >0.85 (as indicated in Fig. 1C, bottom), and the EMG amplitude at that point in time was not more than 2.5 times the template amplitude and not less than the template amplitude divided by 2.5. These highly selective acceptance criteria were designed to result in more false negatives than false positives; for example, the first spike in Fig. 1C was rejected because the correlation coefficient was only 0.79. As the interactive program stepped through the 416 trials, the current template was occasionally replaced with an updated template constructed as the average (Fig. 1C, top right) of all identified spikes in a particular trial (top middle). In examining records of our updated templates, we found that the waveform shape was remarkably stable across the 416 trials, but the amplitude often changed.

As listed in Table 3, unit identification was successful for 30 units in 23 EMG channels (with 1 case where 3 units were identified in the same channel and 5 cases where 2 units were identified in the same channel). An EMG recording was considered to be unacceptable for unit identification if visual inspection of the first 52 trials revealed no clear template or trial-by-trial inspection of the template matches (see Fig. 1C) indicated that two different units were matched by a single template.

DISCRIMINANT ANALYSIS. One way to evaluate the reliability of multiunit EMG patterns is to subject these data to discriminant analysis. We applied this analysis to the normalized, averaged multiunit EMG amplitudes, for the purpose of evaluating the information about hand shape contained in a particular set of EMG data. Thus for each trial, we attempted to classify the set of multiunit EMG levels for the seven muscles as belonging to the true set for a particular object or letter.

We used standard procedures for discriminant analysis as described in more detail in previous publications (Jerde et al. 2003b; Santello and Soechting 1998). Briefly, given a training set of grouped data (i.e., the 7 EMG levels for each trial grouped by object or letter), discriminant analysis maps these data into a multidimensional space (1 dimension for each measured variable) and defines axes in this space that best maximize the ratio of between groups variance to within groups variance. The groups were formed by omitting the trial to be classified, and that trial was then classified as belonging to the closest group.

PRINCIPAL-COMPONENTS ANALYSIS. We used principal-components analysis to find the patterns of covariation across the 17 joint angles (“postural synergies”) and across the seven muscles (“muscle synergies”). For joint angles, this analysis was described in more detail in our previous publications (Jerde et al. 2003a; Santello et al. 1998). The procedure for the EMG data was similar. If EMG_k is the vector composed of the seven multiunit EMG levels for a particular

trial, for each trial (k), the EMG vector can be reconstructed by multiplying the weighting coefficients (EMGwc) by the PCs (EMGpc) and adding

$$\text{EMG}_k = \text{EMG}_{\text{ave}} + (\text{EMGwc}_k1 * \text{EMGpc1}) + (\text{EMGwc}_k2 * \text{EMGpc2}) \dots + (\text{EMGwc}_k7 * \text{EMGpc7})$$

Thus the total seven-muscle pattern for each hand shape can be thought of as a sum of the average plus the weighted combination of seven muscle synergies.

FINDING NEW HAND-SHAPE PCS (HSNC'S) TO FIT EMGPC'S. Because the initially calculated PCs are not necessarily collinear with biologically meaningful patterns, we developed a method to align EMG and hand-shape PCs with one another. Using data sets from the 416 trials of each session, first we took the weighting coefficients of EMGpc1 (EMGwc1) and performed multiple regression with the weighting coefficients for the hand-shape (HS) PCs (HSwc1 through HSwc17)

$$\text{EMGwc1} = b_0 + (b1 * \text{HSwc1}) + (b2 * \text{HSwc2}) \dots + (b17 * \text{HSwc17})$$

This procedure revealed the extent to which the first muscle synergy (EMGpc1) was present in the same trials as each of the postural PCs. For example, if the muscle activations characterized by EMGpc1 produced the postures defined by HSpc2, then the $b2$ weighting coefficient would be close to one and the other weighting coefficients would be close to zero. Thus the regression provided a new set of weighting coefficients ($b1, b2, \dots, b17$) with which to construct a hand-shape "new component" (HSnc)

$$\text{HSnc1} = (b1 * \text{HSpc1}) + (b2 * \text{HSpc2}) \dots + (b17 * \text{HSpc17})$$

The resulting HSnc1 was the axis of postural synergy that was best aligned with the first axis of muscle synergy (EMGpc1). Figure 6, A and B, shows an example of this calculation for EMGpc1. This procedure was repeated for EMGpc2 and EMGpc3.

FINDING TWO IDEAL NEW COMPONENTS. The main goal of this study was to examine the activity of individual muscles or of individual motor units as a function of hand shape. We therefore sought to define an ideal two-dimensional (2D) space in which to express hand shape and plot the "tuning curve" of EMG amplitude or unit firing frequency. Thus we examined the group of new hand-shape PCs generated from the first three EMGpc's for all four subjects and both conditions ($3 \times 4 \times 2 = 24$ new components). We then chose, as HSnc1 and HSnc2, the most commonly occurring hand-shape components by searching all possible subgroups for the two with the lowest SD. As explained in RESULTS, we took the average hand shape represented by each group and then slightly rotated these two new components to make them orthogonal (see Fig. 7).

RESULTS

Hand shape: reducing the degrees of freedom

For each of the four subjects, hand shapes were generally consistent across repeated trials with a given grasped object or fingerspelled letter. For example, Fig. 2, top, shows the values of the 17 joint angles for the 16 repeated trials with the long, flat drawer handle (*subject 1*). The fingers were fully adducted ($\text{ABD} = 0$) and the MCP joints were generally more flexed (positive values) than the PIP joints. Because the thumb was not critically involved in grasping this handle, it was not as consistently placed: the thumb was rotated (ROT) under the handle for most trials, but remained aligned with the hand for two trials (see joint angle 1).

The hand shape on each trial can be perfectly reconstructed as a weighted sum of the 17 PCs. As in our previous studies

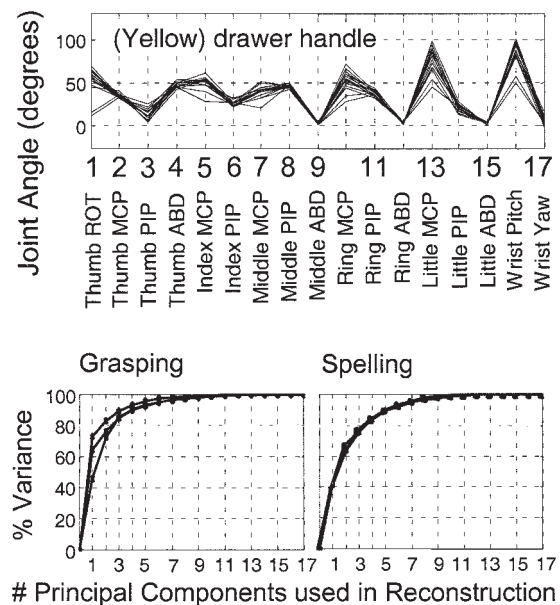


FIG. 2. Hand shapes on individual trials could be reconstructed as a weighted sum of just a few PCs. *Top*: an example of the values of the 17 joint angles in 16 trials where *subject 1* grasped a long, horizontal (yellow) drawer handle as if to pull open the drawer. The fingers were partially extended and fully adducted, and thus the values for abduction (ABD) were close to 0. The thumb was usually rotated (ROT) toward the palm of the hand. Data such as these were used to compute PCs and then to quantify the percent of the variance accounted for by various numbers of components, in a set of 416 trials representing 26 grasped objects (*bottom left*) or 26 ASL letters (*bottom right*). *Bottom*: each line represents 1 subject.

(Jerde et al. 2003a; Santello et al. 1998), we found that these 17 df could be reduced to a much smaller number. Figure 2, bottom, shows the percent variance accounted for by combinations of 1–17 PCs (1, 1 + 2, 1 + 2 + 3, etc.). For grasping (*left*), just two or three PCs accounted for 80% of the variance. For spelling (*right*), because this set of hand shapes was much more diverse, four PCs were needed to account for >80% of the variance.

EMG representations of hand shape

For each trial, we calculated the level of the rectified multiunit EMG (average amplitude across 2 s) for each muscle, as well as the firing frequency of each discriminated single motor unit. The multiunit surface EMG pattern was generally consistent across repeated trials with the same object or letter. Using data from APB and ADM, Fig. 1A displays normalized multiunit EMG levels for the 16 repeats of each object (*left*) or letter (*right*). In Fig. 3, we present examples from individual trials where *subject 1* fingerspelled the letters C, O, or W as well as averages for this subject. The "waveforms" in the *bottom plots* are a convenient way to show the global EMG pattern for each object or letter (these EMG vectors were the inputs to the discriminant and principal-components analyses). The EMG patterns for the C and the O showed only subtle differences because these two hand shapes are very similar. In contrast, the W is an unusual hand shape and was produced with high levels of activity in all of the muscles.

In Fig. 4 and Table 1, we have used discriminant analysis to quantify the information (about hand shape) contained in the static EMG vectors. Figure 4 features two confusion matrices

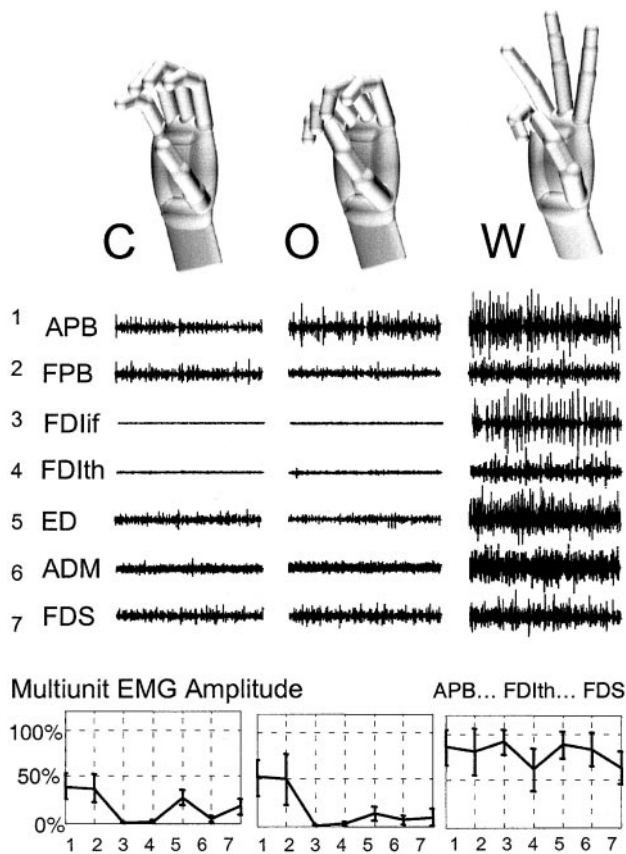


FIG. 3. Rendered hand shapes and muscle activities for 3 American Sign Language (ASL) letters (*subject 1*). Examples from individual trials are shown above plots of the average and SD of the EMG amplitudes across the 16 repeats for the C (*left*) the O (*middle*), and the W (*right*). The C and the O were associated with very similar patterns of muscle activity; the W was quite distinct. See Fig. 1B for definition of the abbreviations for the 7 muscles.

for one subject: grasping results (*left*) and spelling results (*right*). In these plots, the shading in each square represents the number of trials that were classified as a given hand shape, based on the EMG pattern (white = 0 trials, black = 16 trials). A black stripe across the diagonal would represent perfect classification; this was more nearly achieved for spelling than for grasping. The arrows indicate the classification results for the letters and objects mentioned in the preceding text. For spelling, the C was sometimes misclassified as an O and vice versa. For example, Fig. 4 shows that the “actual letter” C (*x* axis) was classified 11 times as C (*y* axis) and 3 times as O (arrow). For grasping, only the (yellow = Y) drawer handle, a relatively distinct hand shape, was perfectly classified based on the EMG pattern.

Table 1 summarizes the results of discriminant analyses for the eight recording sessions (4 subjects, grasping or spelling). Discrimination based on the 17 measured joint angles (*left*) is compared with discrimination based on the EMG pattern (*right*). As expected, the 17 joint angles yielded higher overall rates of correct classification (ranging from 77 to 95%). EMG patterns, however, provided classification at much better than the chance level (4% chance level compared with ~50% correct classification). As also illustrated in Fig. 4, classification was more successful for spelling than for grasping.

EMG principal-components analysis

Thus the multiunit surface EMG pattern was reproducible across trials and was faithfully associated with particular hand shapes. Given these results, it was of interest to examine the main patterns of coactivation or reciprocal activation (positive or negative covariation) among the 7 muscles. To this end, for each subject, the entire set of EMG vectors for the 26 letters (e.g., Fig. 3, *bottom*), or for the 26 objects, was subjected to a principal-components analysis.

As explained in METHODS, the first step in our EMG PC analysis was to subtract away the average multiunit EMG level in each muscle. Thus each EMG pattern was converted to EMG values that ranged positive and negative around the average levels recorded in that session. This is analogous to the procedure used for the analysis of hand shapes, where joint angles varied in both directions around the average joint angles. Thus both the hand shape and the EMG PC “waveforms” can contain positive and negative values (see Figs. 5–7).

The PCs resulting from the EMG PC analysis can be thought of as muscle synergies. As might be expected, the exact waveforms corresponding to EMGpc1 to -3 differed across subjects and even across the two recording sessions (grasping and spelling) for a given subject. For example the first three grasping and spelling PCs for *subject 1* are shown on the right side of Fig. 5.

In Fig. 5, the EMG PCs are represented as static EMG levels in the thumb muscles (APB and FPB), the index finger muscle (FDIif and FDIth), the extrinsic extensor (ED), the little finger muscle (ADM), and the extrinsic flexor (FDS). In examining the entire set of EMG PCs for all subjects, we made the following general observations: 1) a pattern of coactivation across all muscles was found among the first few PCs (EMGpc1–EMGpc3) for all subjects and sessions. In Fig. 5, this pattern is represented by EMGpc1 (solid line) for spelling and by EMGpc2 (dashed line) for grasping. 2) A pattern of reciprocal activation across mechanically distinct muscles was also commonly observed. This occurred most frequently between the thumb muscles and the index finger muscle, i.e., APB and FPB were activated in a manner opposite the two portions of the index finger muscle (FDIif and FDIth). This was seen in EMGpc3 (dotted line) for spelling, and in EMGpc1 (solid line) for grasping. A less pronounced reciprocal pattern sometimes appeared in the four-finger extensor (ED) and flexor (FDS) (also seen in EMGpc1 for grasping).

In Fig. 5, *left*, we show (for all subjects and recording sessions) the percent variance accounted for by various numbers of EMG PCs. Three PCs were needed to account for ~80% of the variance. However, especially because the two FDI electrodes were placed on the same muscle and the two thumb muscles were very close together, this reduction in degrees of freedom (from 6 or 7 to 3) was not nearly as impressive as in the case of the 17 joint angles (cf. Fig. 2). Furthermore in all subjects and sessions (even in the 2 cases where FPB or ADM was missing, and there were therefore only 6 components), the curve was very gradual, indicating a progressive improvement in the reconstruction of the pattern as each synergy is added.

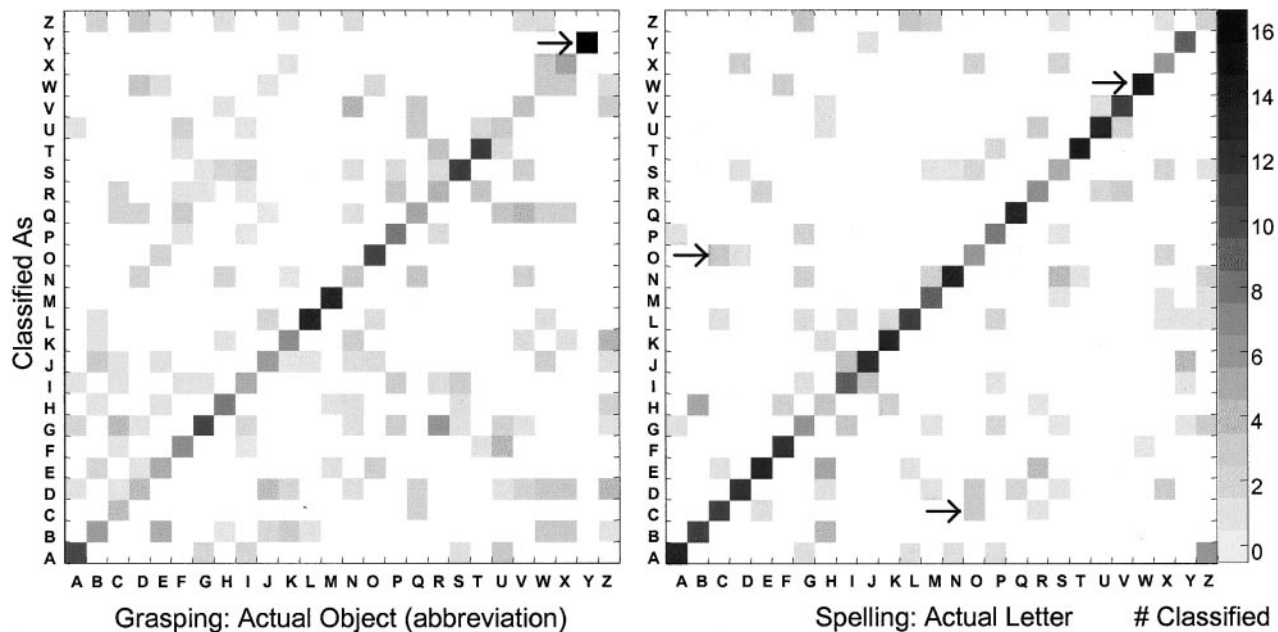


FIG. 4. Confusion matrices show that EMG patterns could be used to correctly identify the object grasped (*left*) or the letter spelled (*right*) on about half of the trials (*subject 1*). The discriminant analysis classification result (*y* axis) is plotted against the actual object or letter (*x* axis), with the number of trials classified shown in gray scale. A black stripe on the diagonal would indicate that all 16 trials were correctly classified. Arrows indicate correct classification for the (yellow = Y) drawer handle and the letter W, and incorrect classification results for the C (classified as O) and the O (classified as C).

Alignment of EMG and hand-shape components

Our main objective was to examine the tuning curves for multi- and single-unit EMG activity as a function of hand shape. As explained in the INTRODUCTION, we used as a starting point the recent discovery of a concise coordinate system for complex hand shapes. One approach would be to adopt the first two hand-shape PCs (HSpc1 and -2) originally calculated for each recording session, as our orthogonal coordinates. However, as in our previous studies, the initially calculated HSpc1 and HSpc2 were not identical across subjects. [Santello et al.

(1998) rotated the PCs of one subject into alignment with the others, and Jerde et al. (2003a) found common PC hand shapes but in various rank orders.] Furthermore, it is well known that the initially calculated PCs, although they have the advantage of being orthogonal, do not necessarily align themselves with the most physiological patterns of covariation (see Flanders and Herrmann 1992).

In light of these considerations, we sought to transform our initial hand-shape PCs into the single, orthogonal, two-dimensional coordinate system that was best aligned with the most commonly observed EMG PCs. Our goal was to find the geometric space of hand shape that was most appropriate for an interpretation of EMG patterns.

Figure 6 illustrates our procedure for bringing hand-shape patterns into alignment with EMG patterns. The figure shows EMGpc1 for *subject 2*'s spelling (Fig. 6A) as well as rendered pictures of the average new first (Fig. 6B) and second (Fig. 6C) hand-shape components (obtained using data from all subjects—see Fig. 7). In the scatter plot (Fig. 6A), each trial is associated with a weighting coefficient for EMGpc1 (*y* axis) and a corresponding value predicted by a multiple regression analysis with the original hand-shape data (*x* axis; see METHODS). A new component (Fig. 6B) was then derived using the b_0 – b_{17} weighting coefficients. Thus the hand-shape new component (HSnc1) was a linear combination of the original hand-shape PCs.

Figure 6, A and B, illustrates how HSnc1 defines the axis of extension-flexion and abduction-adduction that corresponds to the addition or subtraction of the EMGpc1 pattern to the average EMG levels. The positive version of EMGpc1 (i.e., +1.0 weighting) contains excitation of thumb muscles (APB and FPB), muscles expected to abduct the index and little fingers (FDI and ADM), and the four-finger extensor (ED) but very little activity in the four-finger flexor (FD). Addition of

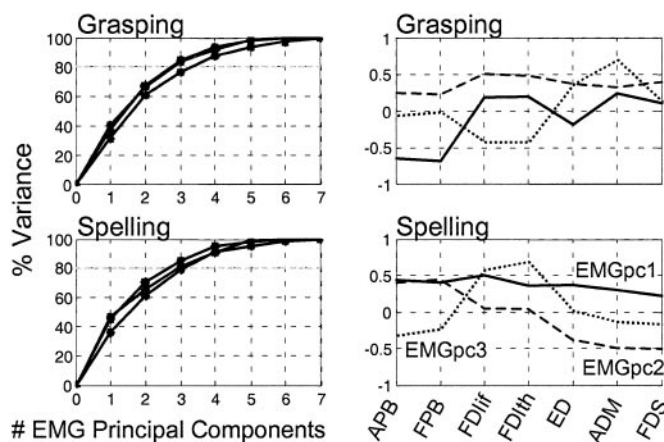


FIG. 5. Percent variance accounted for (*left*) by various numbers of EMG PCs (*right*) for grasping (*top*) and spelling (*bottom*). *Left*: each line represents the results from 1 subject; ~3–4 PCs were needed to account for >80% of the variance, indicating a modest reduction in the degrees of freedom. Two basic patterns of muscle synergy were observed: coactivation of all muscles (all values above the 0 average), and reciprocal activation (above and below the 0 average) between the thumb muscles (APB and FPB) and the index finger muscle (FDI), or between the extrinsic extensor (ED) and flexor (FDS). *Right*: these patterns are exemplified by the 1st 3 PCs of *subject 1*.

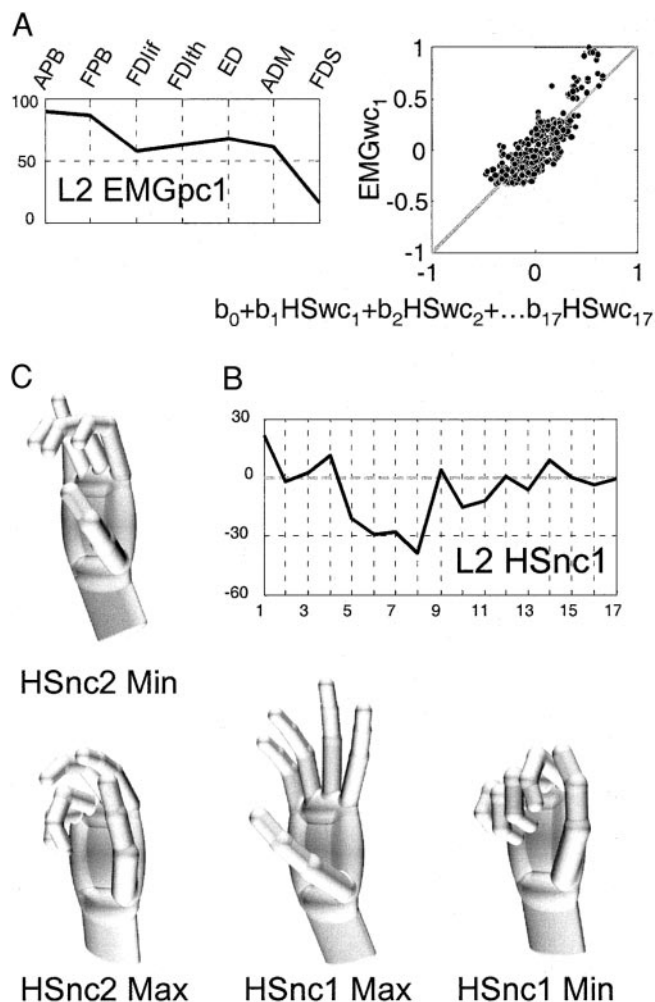


FIG. 6. The 17 PCs of hand shape were recombined to find the new hand-shape components (HSnc's) that corresponded to muscle synergies (EMGpc's). A: the multiple linear regression procedure for finding the proper weighting coefficients (b_0 - b_{17}) to relate the EMGpc1 from *subject 2*'s spelling experiment (left) to the 17 hand-shape PCs from this experiment. B: a plot of the new hand-shape component (HSnc1) that resulted from this procedure as well as a rendering of the maximum (Max) and minimum (Min) values of the average HSnc1 obtained using results from all subjects (see Fig. 7). C: the corresponding renderings for Max (bottom) and Min (top) values of average HSnc2.

this pattern to the average would result in an inwardly rotated thumb and extended and abducted fingers, corresponding to the rendered hand image labeled "Max" in Fig. 6B. Subtraction would amount to substantially below average activity in all muscles except the four-finger flexor (FDS) and would correspond to the neutral thumb location and the partially flexed fingers in the hand image labeled "Min" in Fig. 6B. As discussed in the following text, Fig. 6C illustrates a very different axis of postural synergy (HSnc2).

The procedure illustrated in Fig. 6 resulted in six HSnc's for each subject (3 for each recording session). As shown in Fig. 7, top, we evaluated all possible subgroups of these components and extracted two sets of similar components. Next, the components in each set were averaged to yield just two new components (middle, —). We had to slightly rotate these new components to make them orthogonal (dot product = 0) to one another (middle, ---, and Table 2). The rotation procedure

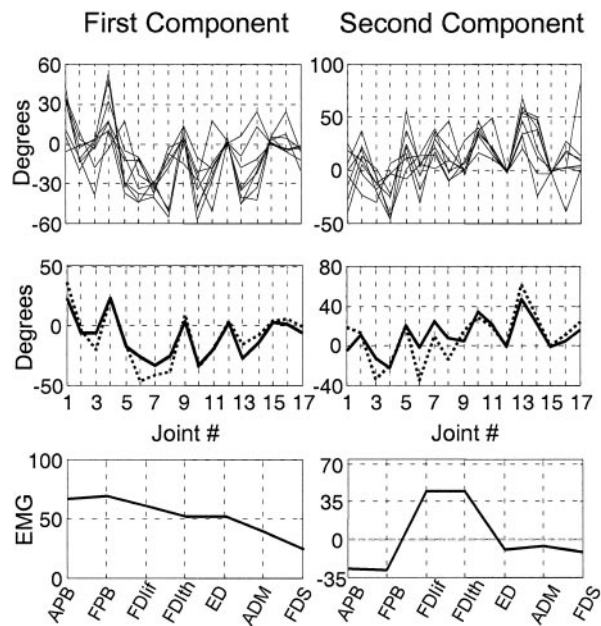


FIG. 7. New hand-shape components that correspond to muscle synergies. Top: groups of similar new components were drawn from the 1st 3 EMGpc's from all recording sessions. Middle: averages of these groups (—) were rotated slightly (---) to make them orthogonal to one another. Bottom: the 2 new hand-shape components correspond to the averages of the muscle synergies from which they were drawn. The 1st muscle synergy exhibited coactivation of all muscles (left); the second muscle synergy exhibited reciprocal activation of the first dorsal interosseous (FDI) with the 2 thumb muscles (APB and FPB).

changed the components very little and did not degrade our ability to discriminate the actual hand shape, using a weighted sum of two components (2-component discrimination was ~50% correct for grasping and ~75% correct for spelling).

In Fig. 7, bottom, we show the average EMG components that correspond to HSnc1 and -2. The first EMG component was a pattern of coactivation across all muscles; the second EMG component was a pattern of reciprocal activation of the thumb and index finger muscles. In subsequent figures, the x

TABLE 2. A two-dimensional coordinate system for hand shape

			HSnc1	HSnc2	Ave
Thumb	1	ROT	36	17	68
	2	MCP	-3	13	20
	3	PIP	-20	-35	27
Index	4	ABD	22	-21	50
	5	MCP	-16	20	36
	6	PIP	-46	-35	43
Middle	7	MCP	-41	8	44
	8	PIP	-38	-14	52
	9	ABD	9	14	6
Ring	10	MCP	-34	29	56
	11	PIP	-18	20	58
	12	ABD	3	0	0
Little	13	MCP	-15	63	49
	14	PIP	-7	29	52
	15	ABD	3	0	-1
Wrist	16	Pitch	5	10	14
	17	Yaw	0	24	-5

Orthogonal hand shape components (HSnc1 and HSnc2) are angles (in degrees) that range positive and negative around the average hand shape (ave). See Fig. 1B for definition of joint angles. HSnc1 and -2, hand shape new components 1 and 2; ROT, thumb rotation; MCP, metacarpal phalangeal; PIP, proximal interphalangeal; ABD, abduction.

axis and the y axes will represent the rotated forms of HSnc1 and -2, respectively. However, one should keep in mind that these axes also represent EMG synergies similar to the averages shown in Fig. 7, *bottom*.

Muscular and motor-unit activation as a function of hand shape

The procedures described in the preceding text resulted in a single 2D coordinate system in which to locate the hand shape for each trial. As illustrated in Figs. 8, 9, and 11, we then used the plots' third dimension (the color scale) to show surface EMG levels or motor-unit firing frequencies. Of course we initially sought to relate the activity of each muscle to the angular excursion of individual joints (using individual linear regressions), but we found that the activity of each of the seven muscles was correlated ($P < 0.001$, $n = 416$) with the trial-to-trial values of ≥ 7 of the 17 joint angles. Thus it seemed more appropriate to view EMG levels as a function of whole-hand shape.

Figure 8, *top*, displays the multiunit EMG levels for *subject 2*'s first dorsal interosseus muscle (FDIif). This panel is also helpful in explaining the "new component" coordinate system

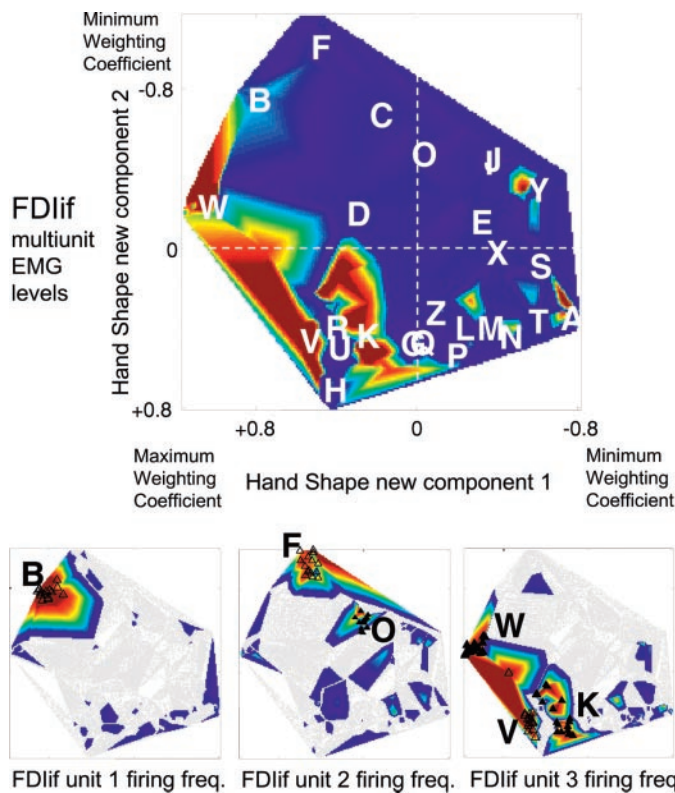


FIG. 8. Multi- and single-unit recruitment profiles for first dorsal interosseus (FDIif). Muscle activity is plotted as the 3rd dimension on a 2-dimensional plot of hand shape. Color coding ranges from the maximum activity in red, to moderate activity in yellow/green, to minimal activity in dark blue. This and subsequent figures used the Matlab "image" and "colormap" functions. Hand-shape axes range from maximum (in the bottom left corner) to minimum, to facilitate comparison with a previous publication (Santello et al. 1998). *Top*: the locations of *subject 2*'s average ($n = 16$) ASL letter hand shapes are indicated on the plot of multiunit EMG levels. *Bottom*: the 3 different motor units discriminated in this muscle had different recruitment profiles. *Color scale*, multiunit = 100–0 normalized EMG units, unit 1 = 16–0 spikes/s, unit 2 = 7–0 spikes/s, unit 3 = 20–0 spikes/s.

because the location of this subject's average hand shapes for each ASL letter are identified on the plot. The x axis ranges from positive (Max) to negative (Min) weightings of HSnc1. As shown in the renderings in Fig. 6B, HSnc1 Max closely corresponded to the hand shape for the letter W (cf. Fig. 3). HSnc1 Min corresponded to the closed hand shapes used for the A, S, T, M, and N (see Jerde et al. 2003b for additional ASL hand shape renderings). For this subject, the hand shapes at the Max extreme of the HSnc2 axis (the y axis) were the V and the H and other letters where index and middle fingers are extended while the other two fingers are flexed. The Min weighting of HSnc2 corresponded to the F, where the index finger was flexed and the other fingers were extended. Thus the HSnc2 axis mainly dissociated the flexion-extension of the four fingers (see rendering in Fig. 6C).

This subject's FDIif multiunit EMG showed peaks corresponding to the letters where the index finger was abducted away from the middle finger. For example the V hand shape resembles the letter itself (with the index and middle finger extended and abducted in a victory sign) and the K is similar except for the placement of the thumb. The W also has an abducted index finger (see Fig. 3).

Three different motor units were discriminated in this FDIif recording (Fig. 8, *bottom*). Not surprisingly, the unit with the largest amplitude waveform (unit 3) exhibited a tuning curve that closely resembled the parent muscle. In the plot for unit 3 (*bottom right*), the small symbols locate individual trials where the subject spelled W, V, or K. In the *bottom, left and middle*, we show the recruitment profiles for two other units recorded on the same electrode. Units 1 and 3 were also recognized in the FDIth (thumb side) recording but with much smaller amplitudes, suggesting that they were mostly contained in the portion of this muscle closer to the index finger (the overall multiunit amplitudes recorded on these two channels were very similar). Unit 2 was also closer to the index finger because it was not recorded on the electrode closer to the thumb.

These three FDIif motor units had very different tuning curves. Unit 1 fired almost exclusively for the letter B. This is an unusual hand shape with the four fingers fully extended and the thumb flexed. Unit 2 fired for the F and the O, both hand shapes in which the index finger tip lightly touches the thumb. Because the unit 3 waveform was larger than that of the other units, it is possible that it obscured recognition of units 1 and 2 in the region of the W, V, and K hand shapes. However, unit 3 did not fire in the regions of the B and O and therefore was distinct from units 1 and 2. Units 1 and 2 had waveforms with comparable amplitudes but had tuning curves that were quite distinct from one another.

In Fig. 9 we show another example of multi- and single-unit data, this time from *subject 3*'s FDS for grasping. As expected, the grasping hand shapes occupied somewhat less of the HSnc2/HSnc1 space. In the *top left*, we locate a few of these hand shapes (averages for *subject 3*). The widely opened hand for grasping the orange juice carton was at the Max extreme of HSnc1 and the Min extreme of HSnc2. Conversely, the more rounded and closed shapes for the rope and comb fell in the opposite corner. This basic distribution is somewhat similar to the results of Santello et al. (1998), who placed the hand shapes for a longer list of objects (57) in the 2D space of the initially calculated PCs (see their Fig. 7).

As will be fully documented in the following text (Table 3),

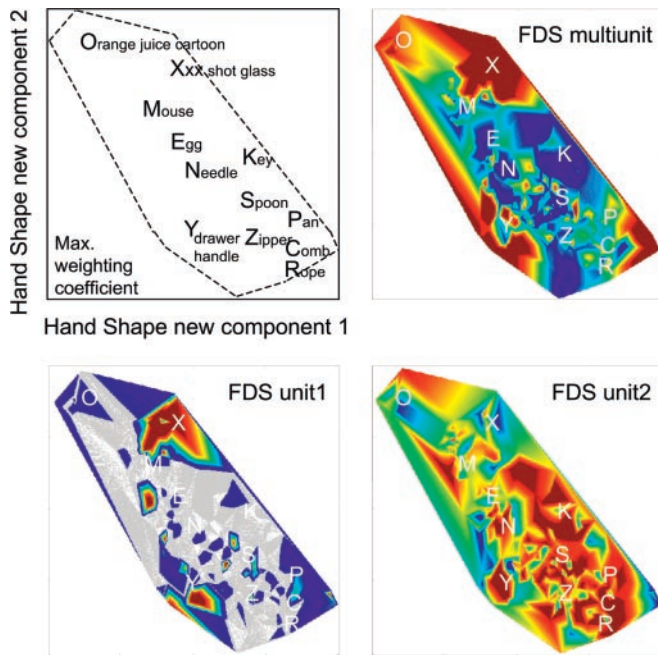


FIG. 9. Multi- and single-unit recruitment profiles for flexor digitorum superficialis (FDS). *Top left*: the locations of some of *subject 3*'s average ($n = 16$) grasping hand shapes are indicated. *Top right*: FDS multiunit activity was high for the Xxx shot glass and the yellow drawer handle. *Bottom left*: FDS unit 1 activity was also high for the Xxx shot glass and the yellow drawer handle. *Bottom right*: a second FDS unit (unit 2) recorded at the same time, had a different recruitment profile. Color scale: multiunit = 100–0 normalized EMG units, unit 1 = 12–0 spikes/s, unit 2 = 16–0 spikes/s.

the vast majority of the identified single motor units had recruitment profiles that resembled the multiunit EMG data from the parent muscle. This was the case for *subject 3*'s FDS multiunit EMG (Fig. 9, *top right*) and FDS unit 1 (*bottom left*). The activity was greatest for the (Xxx) shot glass (where the index and middle fingers were flexed and the ring and middle fingers were extended) and the (yellow) drawer handle (where all fingers were flexed—see Fig. 2). A second FDS unit was recorded at the same time (*bottom right*). Although the waveform amplitudes of units 1 and 2 were similar, and they were sometimes discriminated in the same trials (e.g., for the Pan), their spatial tuning profiles were not well correlated. Instead of being active for the shot glass, unit 2 (*bottom right*) showed its peak activity for the key and the comb (where all fingers were flexed more tightly).

Table 3 quantifies the single-unit results for all subjects and recording sessions. We used the object by object averages to calculate the correlation coefficient of each unit/parent muscle pair. For example, in experiment G1 (Table 3, *top row*), the correlation of data from APB unit1 with data from the parent muscle was highly significant (***) = $P < 0.001$). As illustrated in Fig. 10 (*top left*), the activity of G1 APB unit 2 was also significantly correlated with the parent muscle (***) = $P < 0.001$) as well as with APB unit 1 (** = $P < 0.01$).

As mentioned in the preceding text, the activity of most units ($n = 21$) was highly correlated (***) with the parent muscle. The correlation was weaker in five cases (** = $P < 0.01$, * = $P < 0.05$) and was not significant (NS) in four cases. In most cases where multiple units were discriminated on a single channel, the units' recruitment profiles were not well correlated with one another. Some of these cases were illustrated in Figs.

8 and 9 (L2 FDIif and G3 FDS). This was also true for *subject 3*'s FDIif in grasping (G3) and for *subject 2*'s FDIth in grasping (G2). The EMG records typical of *subjects 1* and *4* made it more difficult to discriminate multiple single motor units. However, it is interesting to note that two of *subject 4*'s thumb motor units (FPB 1 and FPB 2) were better correlated with one another ($P < 0.01$) than they were with the parent muscle ($P < 0.05$ and NS). Thus we have observed a certain degree of motor-unit diversity in three of the four subjects (*subjects 2–4*).

Multiunit EMG as a function of hand shape

The high correlations between multiunit EMG levels and single motor-unit firing frequencies are reassuring, given the inherent difficulty in recording surface EMG from small mus-

TABLE 3. Significance levels for the correlation of 26 average firing rates with the firing rates of other units or with the average surface EMG levels in the parent muscle

Experiment	Correlation With Parent Muscle	Correlation With Other Unit in Same Parent Muscle	
G1			
APB 1	***	**	
APB 2	***	**	
FDIif	***		
ADM	***		
L1			
APB	***		
FPB	***		
ED	***		
ADM	***		
FDS	***		
G2			
FPB	**		
FDIth 1	***	NS	
FDIth 2	**	NS	
ED	***		
L2			
FDIif 1	NS	w/2 NS	w/3 NS
FDIif 2	NS	w/1 NS	w/3 NS
FDIif 3	***	w/1 NS	w/2 NS
G3			
FDIif 1	***	NS	
FDIif 2	NS	NS	
ADM	***		
FDS 1	***	NS	
FDS 2	**	NS	
L3			
FDIif	***	***	
FDIth	***	***	
ED	***		
ADM	***		
FDS	**		
G4			
FPB 1	*	**	
FPB 2	NS	**	
ADM	***		
L4			
FDS	***		

G and L in experiments refer to grasping and spelling, respectively; numbers refer to *subjects 1–4*. APB, abductor pollicis brevis; FDIif, first dorsal interosseus closer to the index finger; ADM, abductor digiti minimi; ED, extensor digitorum; FDS, flexor digitorum superficialis; FDIth, first dorsal interosseus closer to the thumb. *** $P < 0.001$; ** $P < 0.01$; * $P < 0.05$; NS, not significant.

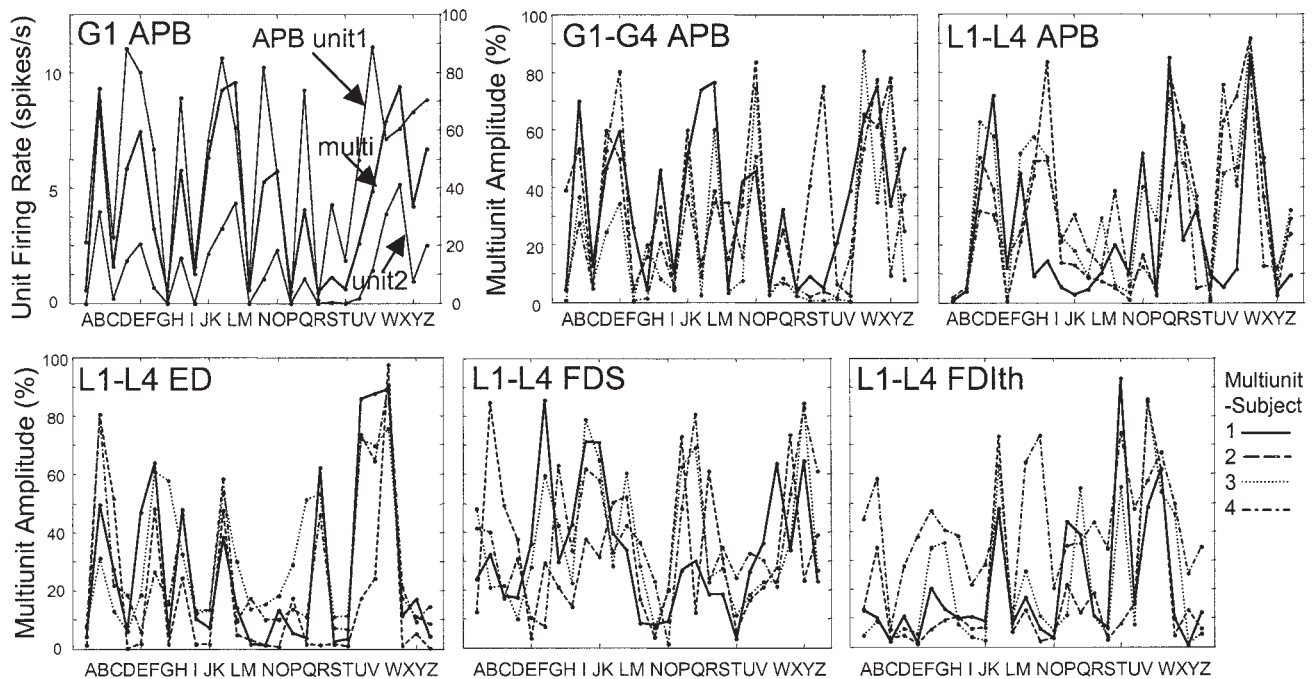


FIG. 10. Average ($n = 16$) multiunit EMG amplitude or single-unit firing rate plotted across the 26 ASL letters (experiments L1–L4) or objects (experiments G1–G4; see Fig. 1A for definition of object abbreviations). *Top left*: the G1 (*subject 1*, grasping) APB multiunit activity (thick line) is compared with the activities of units 1 and 2 (thinner lines). In each of the other panels, the multiunit activity of a given muscle is compared across the 4 subjects (different line types).

cles across a range of postures (see METHODS). Based on their size and proximity to neighboring muscles, recordings from the index finger muscle (FDIif/FDIth), the two thumb muscles (APB and FPB) and the four-finger extensor (ED) should be reasonably free of cross-talk. However, recording from the little finger muscle (ADM) and the four-finger flexor (FDS) is more challenging. Fortunately, we were able to discriminate motor units in these latter two muscles in three of the four subjects (*subjects 1, 3, and 4*, Table 3). In each case, the multiunit EMG was well correlated with the single-unit recruitment profile, tending to validate the results of the multiunit analysis.

Having concluded that our multiunit EMG recordings were robust (Figs. 1A and 4) and highly correlated with single motor-unit data (Table 3), we went on to examine (for each subject and recording session) the global multiunit EMG pattern across all seven EMG channels. In Fig. 10, we show examples from all subjects, and in Fig. 11, we show an example from *subject 1*'s finger spelling as well as a summary of the patterns for all eight recording sessions. The spatial pattern for the thumb muscles (APB and FPB, Fig. 11, *left*) can be compared and contrasted with the pattern for the two portions of the index finger muscle (FDIif and FDIth, Fig. 11, *middle left*). These two muscle groups were coactivated for the abducted and extended hand shapes at the left and top corners of the plot (W and F) but reciprocally activated in the more central region of the plot (D, O, and C; see Fig. 8). This phenomenon of coactivation for some hand shapes and reciprocal activation for others resulted in a relatively low number of sessions with significant correlations across these groups. In Fig. 11, *bottom right*, the gray scale indicates high correlations ($P < 0.001$, $n = 416$) between thumb and index finger muscles in only two to four sessions.

At the opposite extreme, as expected, the patterns recorded from the two electrodes on the FDIif and -th were always highly correlated (in all 8 sessions, black shading in the Fig. 11, *bottom right*). The activity of the four-finger extensor (ED) was often significantly correlated with the activities of all of the other muscles (intermediate gray values on the correlation plot), although the colored-coded recruitment profiles reveal it to be coactivated with FDS and ADM in some regions and reciprocally activated in other regions.

The global recruitment profiles and the muscle/muscle correlations in Fig. 11 echoed the results of the EMG PC analysis presented in Fig. 5. In certain regions, all muscles were coactivated (as in certain PCs), but in other regions, only certain pairs of muscles were coactivated while other pairs were reciprocally activated to varying degrees (as in other PCs). Although these regions and patterns of positive and negative covariation suggest a reduction in degrees of freedom, neither the recruitment profiles nor the results of the PC analysis suggest the presence of a small or discrete number of muscle synergies.

DISCUSSION

When holding the hand in various shapes, the activation of a given intrinsic or extrinsic muscle is related to the positions of numerous joints not just the joints that are directly, mechanically linked to that muscle. This goes along with the observed covariation in the 17 measured joint angles: the 17 dimensional space representing whole hand posture can be reduced to a much smaller dimensionality. This phenomenon allowed us to view muscle or motor-unit activation as a projection onto a 2D coordinate system representing hand shape. These two dimensions were chosen as the hand-shape axes that best corre-

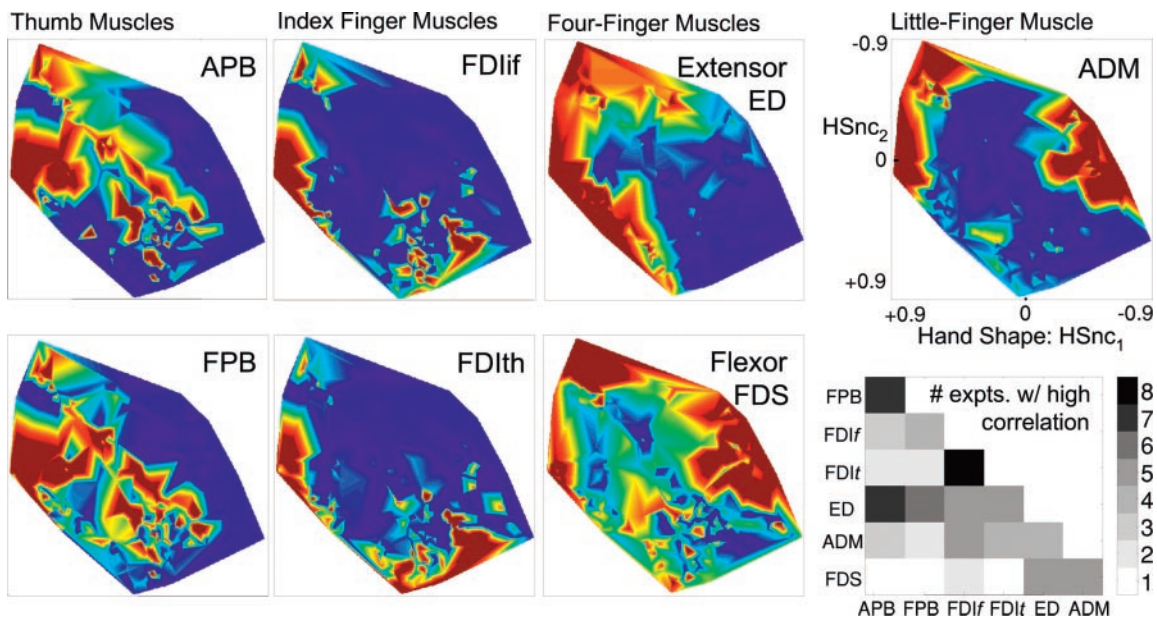


FIG. 11. Multiunit recruitment profiles for all hand muscles recorded from *subject 1* during spelling. The thumb muscles (APB and FPB, *left*) and the index finger muscle (FDI, *middle left*) were coactivated for some hand shapes but reciprocally activated for others. The same was true of the extensor digitorum (ED) compared with the FDS or to the abductor digiti minimi (ADM). *Bottom right*: summary of these results for all subjects, showing (in gray scale) the number of instances, in the 8 recording sessions, where the activities of pairs of muscles were highly correlated ($n = 416$, $P < 0.001$).

sponded to the actions of the most commonly observed muscle synergies. Both multiunit EMG levels and single motor-unit firing frequencies were typically multimodal functions of hand shape, meaning that the recruitment of a typical muscle or motor unit does not align itself with any one axis (be it a single joint rotation, a fixed combination of joint rotations, or an EMG PC). As explained in the following text, this implies that a typical motor unit takes part in multiple muscle synergies.

Muscle synergies

The conclusion that a single muscle may be a member of more than one muscle synergy is in agreement with the results of a series of studies by Bizzi and colleagues (e.g., d'Avella et al. 2003; Tresch et al. 1999). These investigators recorded from several leg muscles while frogs produced forces and movements in various directions. Tresch and colleagues (1999) developed an extraction algorithm to identify the groups of muscles that were active together. They found that the EMG pattern on a particular trial could be represented as a weighted sum of a small number of these muscle synergies, and they suggested that the muscle synergies were the output patterns of discrete control modules in the frog's spinal cord.

The main difference between the synergy extraction algorithm used in the frog studies and the method used here is that our calculation of EMG PCs allowed for reciprocal patterns, where above average activity in one muscle was always accompanied by below average activity in another muscle. Because "synergists" are defined as muscles with similar mechanical actions, the inclusion of reciprocal patterns in "muscle synergies" may seem counterintuitive. However, a muscle synergy is generally thought of a group of muscles that are invariably used together, and therefore if reciprocal activation is part of the normal recruitment/derecruitment pattern, we contend that it is appropriate to allow for its inclusion in a

"muscle synergy." A pattern of excitation of some motor pools accompanied by inhibition of other motor pools is well established for the control of vertebrate locomotion (Engberg and Lundberg 1969; Jankowska et al. 1967), arm movement (Angel 1974), and eye movement (Robinson 1981).

Our EMG PC analysis revealed a reduction in degrees of freedom and highlighted common features across subjects and tasks in the first three EMG PCs. However, as shown in Fig. 5, there was a smooth and gradual improvement as we increased from using two to three to four synergies to account for the variance in the patterns of five or six muscles. If more muscles (such as the lumbricals and the other interosseous and thumb muscles) could have been included in this analysis, they might have joined these three to four synergies, or they might have constituted relatively independent synergies. Furthermore, tasks involving force against the grasped object or movement from one posture to another might involve the main postural synergies reported here or might reveal new synergies. In any case, it appears that there are multiple patterns of covariation across multiple muscles and tasks with the present report providing a lower limit for the quantitative estimate.

As mentioned in the preceding text, the recruitment profiles displayed in Figs. 8, 9, and 11 suggest that it is rare for the activation of a single muscle, or even a single motor unit, to align itself with a single postural or muscle synergy. Because the coordinate axes in these figures were aligned with the main muscle synergies, a simple pattern of membership in a single muscle synergy would appear as a single gradient on this plot or at least as a single peak if the synergy was orthogonal to the two plotted here. The color-scale gradients should be interpreted cautiously because our data points did not uniformly fill the color-coded space. However, in spite of the interpolation between data points, we saw very few instances where the recruitment profiles could be interpreted as unimodal. For

example, in Fig. 8, FDIlf unit 1 has a unimodal tuning curve because it was only active for the B. At the same time, unit 2 cannot be unimodal because it was not active for the C, a letter that falls in between this unit's preferred letters of F and O. Likewise unit 3 cannot be considered unimodal because it was not active for the R, the U, and the H.

Multi- and single-unit EMG tuning curves

Although most people do not use a manual alphabet, holding the hand statically in a variety of shapes is something we all do quite naturally. Additional torques would be needed to produce forces against external objects or to make movements, but a task involving simple postural forces appeared to be a reasonable starting point for our studies. However, in spite of the simplification provided by placing hand shape into a 2D coordinate system, the study of EMG tuning curves for static hand shapes is still more difficult than the study of EMG tuning curves for forces and movements of the proximal arm or wrist.

Perhaps due to the relatively simple mechanics, for the arm and wrist, the activities of motoneurons and motor cortical neurons are well captured by cosine functions of force or movement direction (Amirikian and Georgopoulos 2000; Kakei et al. 1999; Theeuwens et al. 1994). With the arm in a given posture, each motor unit has a single net mechanical action. Muscles with different mechanical actions work together to produce forces in all possible directions, and the pattern is such that a given muscle has a preferred direction of activation near its mechanical action. For force directions geometrically removed from the preferred direction, there is a decrease in the motor units' steady-state firing frequency at a given force amplitude (Theeuwens et al. 1994).

Because in a given posture a given muscle has only one net mechanical action, we were surprised to find that for many proximal arm muscles, plots of EMG level versus force direction were best fit by multiple cosine functions (Flanders and Soechting 1990). We speculated that two peaks in a multiunit EMG tuning curve might result from the combined recording of two distinct populations of motor units (i.e., compartments), each with its own single preferred direction. In fact, Gielen and colleagues had shown that some biceps motor units were preferentially recruited during elbow flexion while others "preferred" supination, and these investigators later reported an analogous result for anterior deltoid (terHaar Romeny et al. 1984; Theeuwens et al. 1994). However, Herrmann and Flanders (1998) showed that these previous results in biceps and deltoid did not necessarily imply a compartmental structure for these muscles. Instead our data revealed that two biceps motor units recorded on the same intramuscular electrode (and presumably in the same compartment) could have significantly different preferred directions. Moreover, we also showed that a single motor unit (in biceps or in deltoid) could have firing frequencies and (task) recruitment thresholds that were best fit by bimodal tuning functions, i.e., a single motor unit could have two preferred directions.

In these previous studies, 2D and three-dimensional (3D) cosine fits to firing frequencies (and linear and planar fits to recruitment thresholds) lent themselves to a relatively simple mechanical interpretation. However, these previous findings for proximal arm muscles are essentially identical to those

reported here for hand muscles: a given muscle or motor unit can have more than one preferred direction.

Implications

Thus single motor units receive a variety of motor commands, and the net result may be that neighboring units in the same muscle are preferentially recruited to produce forces in different directions 3D space or to hold the hand in different static postures. The corollary to this is that a given force or posture involves a collection of units that spans many muscles. Producing a force in a new direction or holding the hand in a new static posture would then entail derecruitment of the current group of motoneurons and recruitment of a new group, which may or may not contain some of the same members as the old group. This scenario is consistent with the one that might be inferred from the distributed anatomical representations of the arm and hand in motor cortical areas (reviewed by Schieber 2001). However, until now it appeared that compared with recruitment at the level of cortical neurons, recruitment at the level of motoneurons was much more simply related to muscle mechanical actions.

From the perspective of motor learning and recovery from injury, a distributed neuromuscular control system has certain advantages. Improvement in performance can occur by gradually tuning the entire network and a discrete lesion would partially disable several synergies instead of knocking out an entire module. However, the more obvious motivation for this type of control scheme may lie in the complex biomechanical architecture of the muscles and connective tissue of the arm and hand. It is impossible to move (or even to produce isometric force) at a single joint without the necessity of balancing unwanted forces at other joints. Thus biomechanical considerations may dictate that large groups of motor units with diverse mechanical actions must be recruited together in highly distributed motor-unit synergies.

ACKNOWLEDGMENTS

The authors thank J. F. Soechting for consultation and K. Simura for comments on the manuscript.

GRANTS

This work was supported by National Institute of Neurological Disorders and Stroke Grant R01 NS-27484.

REFERENCES

- Amirikian B and Georgopoulos AP. Directional tuning profiles of motor cortical cells. *Neurosci Res* 36: 73–79, 2000.
- Angel RW. Electromyography during voluntary movement: the two-burst pattern. *Electroencephalogr Clin Neurophysiol* 36: 493–498, 1974.
- d'Avella A, Santiel P, and Bizzi E. Contributions of muscle synergies in the construction of natural motor behavior. *Nat Neurosci* 6: 300–308, 2003.
- Engberg I and Lundberg A. An electromyographic analysis of muscular activity in the hindlimb of the cat during unrestrained locomotion. *Acta Physiol Scand* 75: 614–630, 1969.
- Flanders M. Choosing a wavelet for single-trial EMG. *J Neurosci Methods* 116: 165–177, 2002.
- Flanders M and Herrmann U. Two components of muscle activation: scaling with the speed of arm movement. *J Neurophysiol* 67: 931–943, 1992.
- Hager-Ross C and Schieber MH. Quantifying the independence of human finger movements: comparisons of digits, hands, and movement frequencies. *J Neurosci* 20: 8542–8550, 2000.

- Herrmann U and Flanders M.** Directional tuning of single motor units. *J Neurosci* 18: 8402–8416, 1998.
- Huesler EJ, Maier MA, and Hepp-Reymond MC.** EMG activation patterns during force production in precision grip. III. Synchronization of single motor units. *Exp Brain Res* 134: 441–455, 2000.
- Jankowska E, Jukes MGM, Lund S, and Lundberg A.** The effect of DOPA on the spinal cord. V. Reciprocal organization of pathways transmitting excitatory action to alpha motoneurons of flexors and extensors. *Acta Physiol Scand* 70: 369–388, 1967.
- Jerde TE, Soechting JF, and Flanders M.** Biological constraints simplify the recognition of hand shapes. *IEEE Trans Biomed Eng* 50: 265–269, 2003a.
- Jerde TE, Soechting JF, and Flanders M.** Coarticulation in fluent finger-spelling. *J Neurosci* 23: 2383–2393, 2003b.
- Johanson ME, Valero-Cuevas FJ, and Hentz VR.** Activation patterns of the thumb muscles during stable and unstable pinch tasks. *J Hand Surg* 26: 698–705, 2001.
- Kakei S, Hoffman DS, and Strick PL.** Muscle and movement representations in primary motor cortex. *Science* 285: 2136–2139, 1999.
- Keen DA and Fuglevand AJ.** Common input to motor neurons innervating the same and different compartments of human extensor digitorum muscle. *J Neurophysiol* 91: 57–62, 2004.
- Kilbreath SL and Gandevia SC.** Limited independent flexion of the thumb and fingers in human subjects. *J Physiol* 479: 487–497, 1994.
- Maier MA and Hepp-Reymond MC.** EMG activation patterns during force production in precision grip. I. Contribution of 15 finger muscles to isometric force. *Exp Brain Res* 103: 108–122, 1995a.
- Maier MA and Hepp-Reymond MC.** EMG activation patterns during force production in precision grip. II. Muscular synergies in the spatial and temporal domain. *Exp Brain Res* 103: 123–136, 1995b.
- Paulignan Y, Frak VG, Toni I, and Jeannerod M.** Influence of object position and size on human prehension movements. *Exp Brain Res* 114: 226–234, 1997.
- Rearick MP, Casares A, and Santello M.** Task-dependent modulation of multi-digit force coordination patterns. *J Neurophysiol* 89: 1317–1326, 2003.
- Reilly KT and Schieber MH.** Incomplete functional subdivision of the human multitendoned flexor digitorum profundus: an electromyographic study. *J Neurophysiol* 90: 2560–2570, 2003.
- Robinson DA.** The use of control systems analysis in the neurophysiology of eye movements. *Annu Rev Neurosci* 4: 463–503, 1981.
- Santello M, Flanders M, and Soechting JF.** Postural hand synergies for tool use. *J Neurosci* 18: 10105–10115, 1998.
- Santello M, Flanders M, and Soechting JF.** Patterns of hand motion during grasping and the influence of sensory guidance. *J Neurosci* 22: 1426–1435, 2002.
- Santello M and Soechting JF.** Gradual molding of the hand to object contours. *J Neurophysiol* 79: 1307–1320, 1998.
- Santello M and Soechting JF.** Force synergies for multifingered grasping. *Exp Brain Res* 133: 457–467, 2000.
- Schieber MH.** Muscular production of individuated finger movements: the roles of extrinsic finger muscles. *J Neurosci* 15: 284–297, 1995.
- Schieber MH.** Constraints on somatotopic organization in the primary motor cortex. *J Neurophysiol* 86: 2125–2143, 2001.
- terHaar Romeny BM, Denier van der Gon JJ, and Gielen CCAM.** Relation between location of a motor unit in human biceps brachii and its critical firing levels for different tasks. *Exp Neurol* 85: 631–650, 1984.
- Theeuwes M, Gielen CCAM, Miller LE and Doorenbosch C.** The relation between the direction dependence of electromyographic amplitude and motor unit recruitment thresholds during isometric contractions. *Exp Brain Res* 98: 488–500, 1994.
- Tresch MC, Saltiel P, and Bizzi E.** The construction of movement by the spinal cord. *Nat Neurosci* 2: 162–167, 1999.
- Valero-Cuevas FJ.** Predictive modulation of muscle coordination pattern magnitude scales fingertip force magnitude over the voluntary range. *J Neurophysiol* 83: 1469–1479, 2000.